Intermetallics 161 (2023) 107960

Contents lists available at ScienceDirect

Intermetallics

journal homepage: www.elsevier.com/locate/intermet

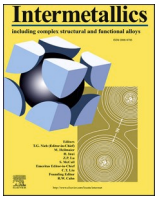

Hybrid molecular dynamic Monte Carlo simulation and experimental production of a multi-component Cu–Fe–Ni–Mo–W alloy

M. Dias [a,*], P.A. Carvalho [b], A.P. Gonçalves [c], E. Alves [a], J.B. Correia [d]

[a] Instituto de Plasmas e Fusão Nuclear, Instituto Superior Técnico, Universidade de Lisboa, Av. Rovisco Pais, 1049-001, Lisboa, Portugal
[b] SINTEF, Forskningsveien, Oslo, Norway
[c] C²TN, Instituto Superior Técnico, Universidade de Lisboa, Campus Tecnológico e Nuclear, Estrada Nacional 10, 2695-066, Bobadela LRS, Portugal
[d] LNEG, Laboratório Nacional de Energia e Geologia, Estrada do Paço do Lumiar, 1649-038, Lisboa, Portugal

ARTICLE INFO

Keywords:
Molecular dynamics
High entropy alloys
Monte Carlo simulation
Microstructure
X-ray diffraction

ABSTRACT

High-entropy alloys are a class of materials intensely studied in the last years due to their innovative properties. Their unconventional compositions and chemical structures hold promise for achieving unprecedented combinations of mechanical properties. The Cu–Fe–Ni–Mo–W multicomponent alloy was studied using a combination of simulation and experimental production to test the possibility of formation of a simple solid solution. Therefore, Molecular Dynamics and hybrid Molecular Dynamic/Monte Carlo simulations from 10K up to the melting point of the alloy were analyzed together with the experimental production by arc furnace and powder milling. The Molecular Dynamics simulations starting with a bcc type-structure show the formation of a single-phase bcc solid solution type-structure, whereas using Monte Carlo one, generally produced a two-phase mixture. Moreover, the lowest potential energy was obtained when starting from a fcc type-structure and using Monte Carlo simulation giving rise to the formation of a bcc Fe–Mo–W phase and a Cu–Ni fcc type-structure. Dendritic and interdendritic phases were observed in the sample produced by arc furnace while the milled powder evidence an separation of two phases Cu–Fe–Ni phase and W–Mo type-structures. Samples produced by both methods show the formation of bcc and a fcc type-structures. Therefore, the Monte Carlo simulation seems to be closer with the experimental results, which points to a two-phase mixture formation for the Cu–Fe–Ni–Mo–W multicomponent system.

1. Introduction

In the last decade, high-entropy alloys (HEA) emerged as a promising new class of materials due to the with remarkable properties achievable. HEA are solid solutions that present desirable properties such as high hardness [1] and resistance to wear [2], oxidation [3] corrosion [4] and irradiation resistance [5], as well as high thermal stability [6]. These materials with increasing atomic size difference prefer the bcc-type-structure over the fcc one, which is originated from the ability of the bcc structure to accommodate a large atomic size difference with lower strain energy [7]. The distortion or fluctuation in the lattice is one of the main characteristics of HEA which is related to the sluggish diffusion kinetics in the materials. Moreover, the diffusion coefficients in HEA are lower than those of reference metals due to the fluctuations in the lattice potential energy. This could hamper the formation of intermetallics in the lattice and stabilize the solid solution [8]. To date, many different HEA systems have been investigated, which typically include Fe, Al, Cu, Ti, Mg, and Ni [9]. The use of refractory-element based HEA (Mo, Nb, Ta, W and V) was introduced by Senkov et al. [10] mainly as candidates for structural applications at temperatures above 1373K. Many other refractory HEAs were subsequently developed to obtain improved strength, room temperature ductility and high hardness up to 1873K [11]. In the last years the investment on high entropy alloys is growing and refractory single phase high entropy was achieve as TiVCrNiZ [12] as well as low density one as MgAlMnFeCu [13] and transitions metals one as CrMnFeCoMo [14]. Heavy alloys have included a combination of either W–Ni–Cu or W–Ni–Fe and Mo has been used as alloying element as well [15]. It seemed thus, that an equimolar high entropy alloy of these five elements was worth testing within the scope of searching for HEAs in the context of heavy alloys/tungsten applications.

Molecular dynamics (MD) is a simulation technique for computing

* Corresponding author.
E-mail address: marta.dias@ctn.tecnico.ulisboa.pt (M. Dias).

https://doi.org/10.1016/j.intermet.2023.107960
Received 31 January 2023; Received in revised form 22 May 2023; Accepted 27 May 2023
Available online 23 June 2023

the equilibrium and transport properties of a classical many-body system, where each atom is assumed as a point mass, and the atomic motion is based on the Newton's equation [16]. In addition, for describing the interaction between the elements it is used an embedded atom method (EAM) potential that is extensively used for metals [17]. Such a potential is non-pairwise in the sense that it is based on concepts [16] from density functional theory, which stipulate in general that the energy of a solid is a unique function of the electron density and correlate well with more precise bonding methods [18]. The Metropolis-Monte Carlo simulation method is an alternative to the molecular dynamics one. Its basis is the random swapping of atoms positions in pursuit of a more stable overall configuration. Recently, hybrid molecular dynamics-Monte Carlo (MC) simulation have been used for simulating HEAs [19]. The LAMMPS software [20] from Sandia Labs can perform both MD and MC simulations in materials using a EAM potential as well as simulate X-ray diffraction patterns from atomistic simulation results [21]. This work presents Molecular Dynamics and Monte Carlo simulations for the system Cu–Fe–Ni–Mo–W as well as the experimental evidence which could confirm the simulations. This set of chemical elements is representative of typical heavy tungsten alloys and include both W and Cu, also typical elements used in plasma facing structures for nuclear fusion applications.

2. Experimental details

An equimolar CuFeNiTaW alloy was simulated using periodic boundary conditions. The software LAMMPS of Sandia Labs was used for a) Molecular Dynamics b) hybrid Molecular Dynamic/Monte Carlo simulations and c) simulated X-ray diffraction of MD and MC simulated materials. For bcc simulations (13^3 cells), the number of atoms was 4394 and for fcc simulations (10^3 cells) the number of atoms was 4000. The typical sequence of simulation involved several steps of energy minimization of the initial configuration, heating to the simulation temperature and energy minimization for a period of 6×10^6 time steps. The hybrid Molecular Dynamic/Monte Carlo simulation, hereafter referred as MC, consisted in the introduction of a Monte Carlo swap attempt every 10 Molecular Dynamic simulation steps. The temperature used in the Metropolis criterion dictating swap probabilities was the same of the isothermal MD simulation. Pressure was maintained at 1 atm. The EAM potential for Cu–Fe–Ni–Mo–W was retrieved from NIST [22] referring to the original work of Zhou et al. [23]. The same procedure, using the same data set for simulation of a binary alloy, has been reported in the literature [24].

Apart from the simulation studies, there was also experimental work, with the Cu–Fe–Ni–Mo–W samples being prepared using arc-furnace and ball milling. First, a Cu–Fe–Ni–Mo–W composition sample (each element with 99.9% nominal purity and average particle size of 10 μm, AlfaAesar) was weight and melted in an arc furnace equipped with a cold crucible under an argon atmosphere. In order to increase the homogeneity of the sample, a pellet containing a homogeneous mixture of the elements was prepared before used in the melting. The alloys were melted at least three times to ensure homogeneity, before quenching to room temperature. The mass loss during processing was below 1 wt%.

Powders of Cu, Ni, Fe, Mo and W (99.9% nominal purity with average particle size of 10 μm, AlfaAesar) were mixed in an equiatomic proportion and mechanically alloyed inside a high-energy planetary Restch EMAX mill, with 1 cm steel balls and steel vials. The balls to powder mass ratio was 10:1, and the milling occurred for 4 h at 1200 rpm. Powder X-ray diffraction measurements of the arc furnace samples were performed at room temperature using monochromatic Cu K_α radiation in a Panalytical X'Pert Pro diffractometer with a 2θ–step size of 0.02° from 20° to 80°. Moreover, the milled powder was analyzed using a PANalytical Empyrean diffractometer in reflection geometry, using Cu $K_{\alpha 1}$ radiation and a step size of 0.013°. Metallographic preparation of the samples was performed by grinding with SiC paper, polishing with diamond suspensions of 6 μm, 3 μm and 1 μm nominal grain size, and final fine polishing with colloidal silica suspension of 0.2 μm granulometry. The microstructures were observed before and after irradiation by secondary electrons (SE) and backscattered electrons (BSE) imaging using a JEOL JSM-7001F field emission gun SEM. The transmission electron microscopy (TEM) work was performed with a DCOR Cs probe-corrected FEI Titan G2 60–300 instrument with 0.08 nm of nominal spatial resolution. Chemical information was obtained by X-ray energy dispersive spectroscopy (EDS) with a Bruker SuperX EDS system, comprising four silicon drift detectors. STEM samples were prepared using a Ga^+ focused ion beam with a Thermofisher Helios G4 dual beam instrument.

Table 1
Thermodynamic calculations for Cu–Ni–Fe–Mo–W system.

Composition	ΔH_{mix} (kJ/mol)	δ × 100	VEC
CuNiFeMoW	7.04	4.25	8.20

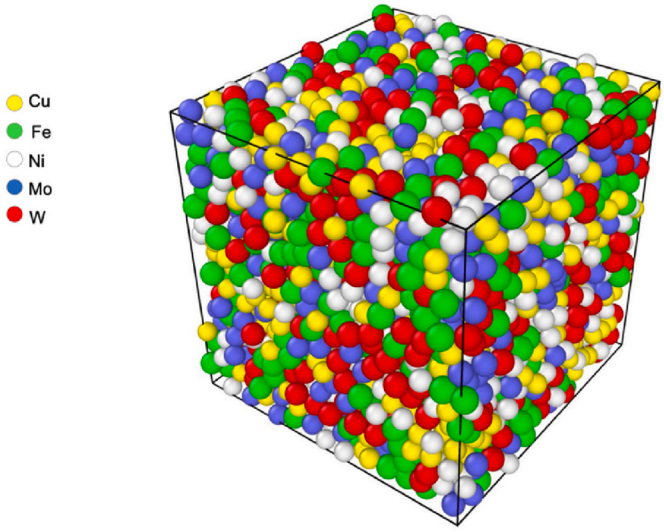

Fig. 1. Molecular dynamics started from random positions at 300K.

Simple thermodynamics calculations were performed to anticipate the structures resultant from the alloying process and helping with the interpretation and discussion of the results. Based on empirical models [25,26], using the enthalpies and entropies of mixing, ΔH_{mix} and ΔS_{mix}, the percentual atomic size differences, δ, and the valence electron concentrations, VEC, it is possible to predict what solid solutions tend to form in the ranges -15 kJ/mol $\leq \Delta H_{mix} \leq 5$ kJ/mol, $1 \leq \delta \times 100 \leq 6$ with the most stable phases being predominantly fcc at VEC $\geq$8 and bcc at VEC $<$6.87. Between these values, mixed fcc and bcc-type phases are expected to coexist. In this context, calculations of the relevant parameters of Cu–Ni–Fe–Mo–W system are presented in Table 1. Based on the calculated values, no solid solutions can be expected for this composition.

3. Results and discussion

Since the thermodynamical calculations did not predict the formation of a single solid solution, the simulation was started from a random distribution of the five elements either with bcc or fcc type-structures as presented in the next sections, considering for each type of crystal structure one of the simulation models: molecular dynamics (MD) or Monte Carlo (MC).

3.1. Simulation starting from random positions

An initial attempt for simulation in this system was generated from a

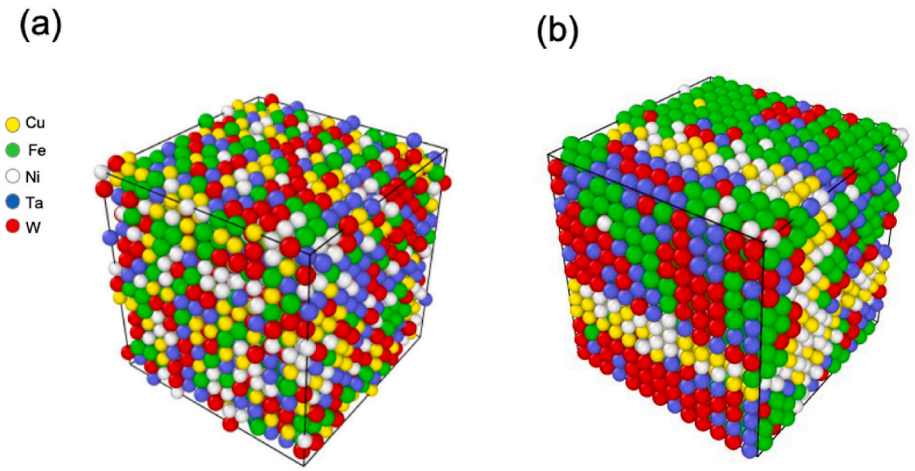

Fig. 2. (a) Molecular dynamics and (b) Monte-Carlo simulations started from bcc type-structure at 300K.

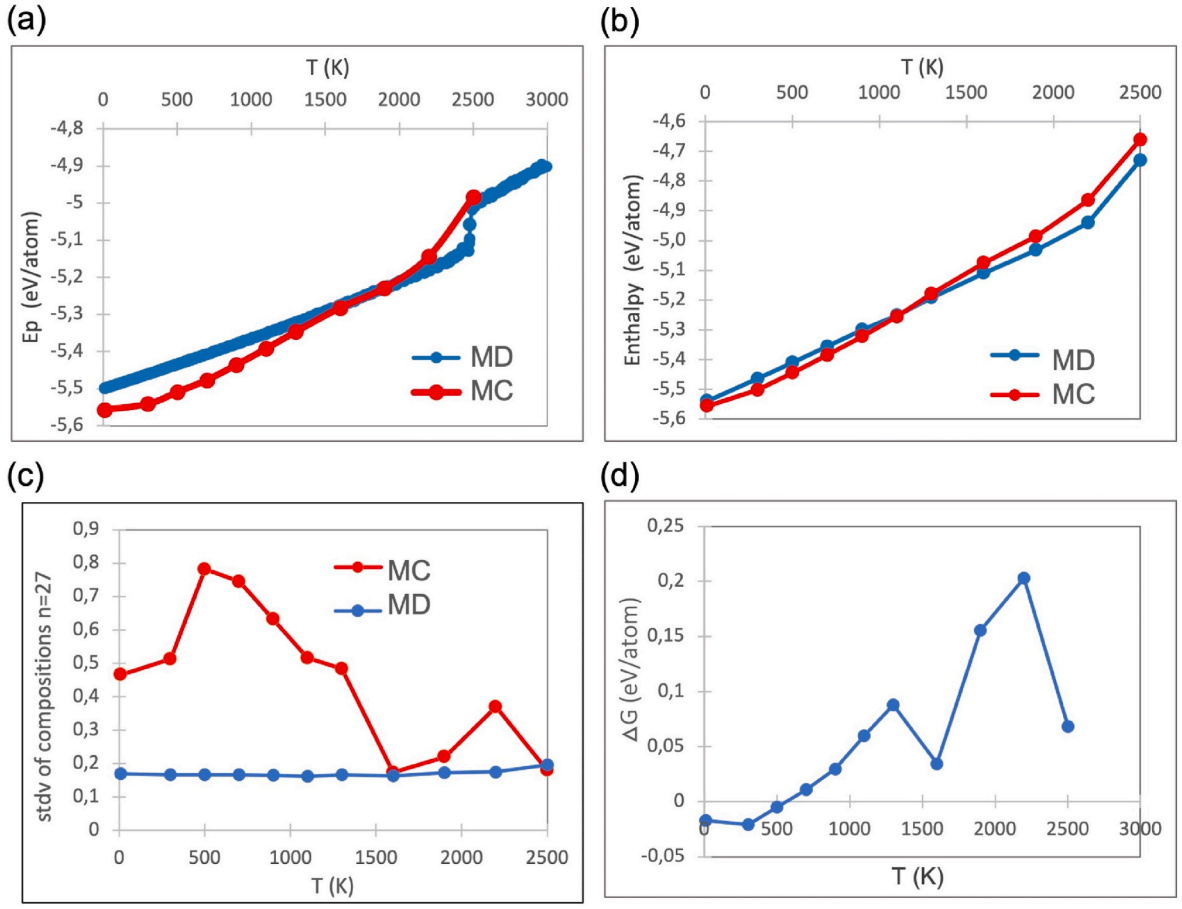

Fig. 3. (a) Potential energy versus temperature calculated starting from bcc via MD and MC and (b) Enthalpy versus temperature calculated via MD and MC simulations, (c) chemical segregation versus temperature as measured from analyses on a grid of 27 locations in each simulation and (d) calculated difference in free energy between a single phase structure (MD) simulation and a two phase structure (MC) simulation.

set of random atom positions and elements distribution. This arrangement of starting configuration was very far from the usual crystalline lattice. It was thought that with careful MD simulated cooling for 6×10^6 time steps from 2500K, above the melting temperature of the alloy, to 10K followed by annealing using MC procedure for an additional 6×10^6 time steps, e.g. at 300K, crystallization might arise. In fact, there was no evidence of crystallization (Fig. 1) and the alloy remained in an amorphous state. Hence, new starting structures were chosen for the simulation, namely fcc and bcc type-structures, as these are the most probable outcomes for this type of alloy system.

3.2. *Simulation starting from a bcc type-structure*

Fig. 2 shows the results for (a) molecular dynamics (MD) and (b) Monte Carlo (MC) simulations for the Cu–Fe–Mo–Ni–W multi-component high entropy alloy at 300K starting with a bcc type-

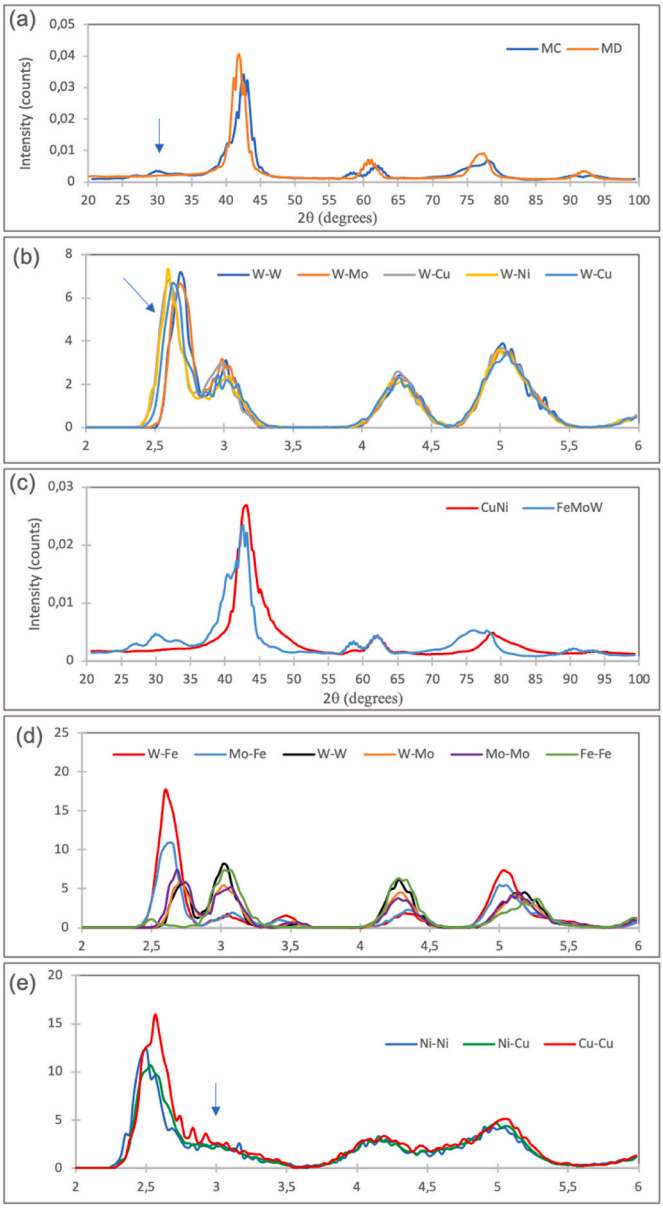

Fig. 4. (a) Simulated XRD from MD and MC simulations starting from bcc at 300K (b) Partial radial distribution function (RDF) for several types of bonds in the MD simulation at 300K (c) Simulated XRD from MC simulations at 300K obtained separately from the two segregated phases. (d) Partial radial distribution function (RDF) for several types of bonds in Fe–Mo–W phase of the MC simulation at 300 K (e) Partial radial distribution function (RDF) for several types of bonds in Cu–Ni phase of the MC simulation at 300 K. The arrows in (a) show the presence of peak at 30°, in (b) represented curves which are typical of a bcc type-structure and in (d) evidence the first peak which correspond to Fe.

structure. A uniform distribution of elements was found using the MD simulation while a separation into two phases Fe–Mo–W and Cu–Ni are presented for MC.

Fig. 3 exhibits the variation of (a) potential energy and the (b) enthalpy of formation as a function of temperature for both simulations. Both the potential energy and the enthalpy were obtained directly from the LAMMPS simulation. The presented values in Fig. 3, correspond to the end of the simulation after 6 million timesteps. The results show that at temperatures lower than 1500 K, MC simulation has a more negative potential energy and enthalpy of formation than MD simulation. For each simulation, the chemical segregation was measured on a grid of 27 locations in the simulation cell, each analyzing a 9 nm diameter sphere of the lattice. The standard deviation of these measurements are shown in Fig. 3 (c). The MD simulations produced a uniform solid solution (blue curve in Fig. 3 (c)) with an almost flat curve with the values constant. In contrast, MC simulations produced much more segregated phases. At high temperatures due to thermal agitation, MC simulations tend to be less segregated and, close to the melting temperature ~2500K all simulations coincide with the lower value of segregation corresponding to the liquid state. Fig. 3 (d) exhibits the calculated difference in free energy between a single phase structure, obtained with MD simulation, and a two phase structure, obtained with MC simulation, i.e. $\Delta G = G$ two phases (MC)-G single phase (MD). This corresponds in general to the difference between a two phases separation, the typical result of this MC simulation and, a uniform solid solution, the common result of MD only simulation. It was assumed for this calculation that only configurational entropy (segregated vs uniform) contributes to free energy which was verified experimentally [23]. Therefore, it is predicted from the evaluation of free energy as function of temperature simulation that a two-phase segregated structure will be more stable in the Cu–Fe–Mo–Ni–W multi-component system at low temperatures, up to 500K, whereas at higher temperatures a true solid solution is expected when starting from a bcc type crystal structure.

The XRD pattern simulation is shown in Fig. 4 (a) at 300 K using MC and MD calculations. A basic bcc type-structure pattern is evidenced for the MD simulation with a lattice parameter of 3.02 Å. However, the structure configuration established via MC can be interpreted as a tetragonal distortion as well as extra reflection around $2\theta = 30^{o}$ (see the arrow in Fig. 4 (a)) compatible with the B2 type-structure with the same lattice parameter.

The partial radial distribution function (RDF) for several types of bonds corresponding to the MD simulation at 300K is presented in Fig. 4 (b). The represented curves are typical of a bcc type-structure although the distance of the first neighbor varies significantly with the chemical element (see the arrow in Fig. 4 (b)), since the curves are not overlapped, indicating a significant degree of micro distortion in the lattice. This is a common feature in HEAs [27]. In a HEA local distortions reached 3%, although mean values for the alloy were modest ~0.1% [28]. The analysis of the XRD calculated from MC simulations at 300K obtained separately from the two segregated phases, Fig. 3 (c), clearly shows that both the tetragonal distortion and the B2 type-structure extra reflection are associated with the Fe–Mo–W phase. The partial radial distribution function (RDF) for several types of bonds in Fe–Mo–W phase presented in Fig. 4 (d). It shows that the first peaks, correspondent to Fe bonds, are at shorter distances than those of the other elements. Therefore, this is evidence that the bond lengths involving Fe atoms are shorter than those involving Mo and W. This may be the reason for the existence of the tetragonal shift identified in the MC simulation at 300K. Moreover, the RDF of Cu–Ni phase shown in Fig. 4 (e) evidence the absence of a clearly defined second peak around 3 Å (see the arrow in Fig. 4 (e)). This is not an unusual feature in HEAs, for instance it has been verified experimentally before using neutron and X-ray diffraction [29]. This is nevertheless a minor effect; using the common neighbor analysis of OVITO software on the MC at 300K simulation a 99% bcc type-structure is detected.

3.3. *Simulation starting from a fcc type-structure*

Fig. 5 shows the results for (a) and (b) molecular dynamics (MD) and (b) and (c) Monte Carlo (MC) simulations for the Cu–Fe–Mo–Ni–W multi-component high entropy alloy at 300K starting with a fcc type-structure. Using MD only there is no chemical segregation, (Fig. 5 (a)), and the final structure is fully a bcc. A fast phase transition from fcc to bcc is observed for final configurations of MD simulations and the final chemical segregation is not very different from that of the simulation starting with a bcc type-structure. However, as the starting simulation cell structure was fcc and the bcc type-structure was formed by local nucleation, a polycrystalline structure was formed. Fig. 5 (b) depicts the

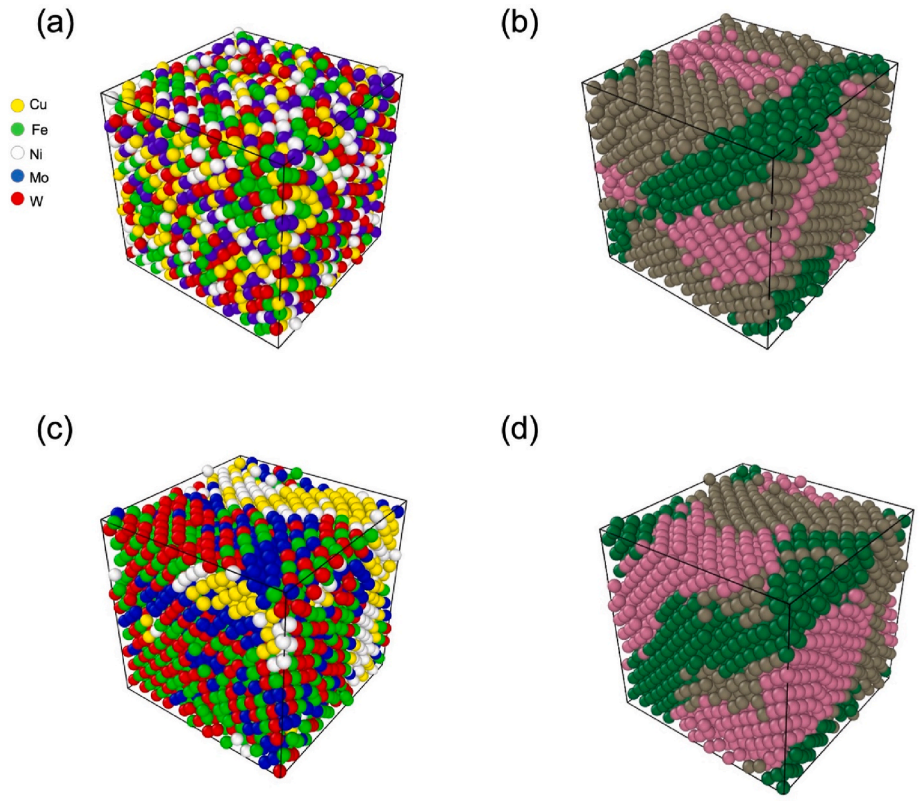

Fig. 5. Simulations started from fcc type-structure at 300K (a) and (b) Molecular dynamics and grain segmentation (c) and (d) Monte-Carlo and grain segmentation. In (d) the brown atoms indicated fcc grains and the remainder are bcc.

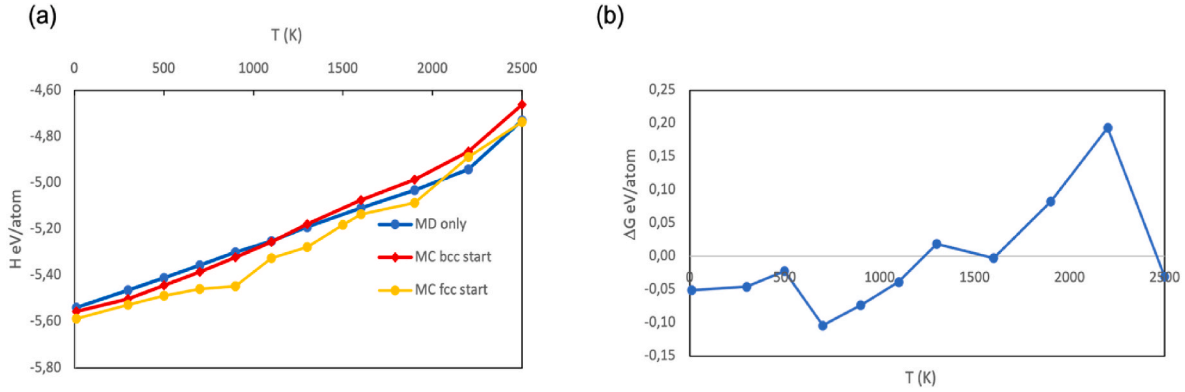

Fig. 6. (a) Enthalpy versus temperature starting from fcc calculated via MD and MC simulations and (b) calculated difference in free energy difference in free energy between a single phase structure (MD) simulation and a two phase structure (MC) simulation.

grain segmentation obtained via lattice orientations using the OVITO software [30]. The MC simulation starting from a random distribution of elements in a fcc type-structure yielded two phases: a bcc type-structure constituted by Fe–Mo–W and a fcc phase constituted by Cu–Ni (Fig. 5 (c)). A fast phase transition from fcc to a major bcc and a minor fcc phases was observed for final configurations of MC simulations. The final chemical segregation is not very different from that of the simulation starting with a bcc type-structure, however when starting from a fcc crystal in the simulation cell the segregated Cu–Ni phase also shows a distinct fcc type-structure, brown phase (Fig. 5 (d)).

A decisive parameter for microstructure selection is the free energy. Fig. 6 shows the enthalpy for MC and MD simulations starting from fcc and the calculated difference in free energy between MC and MD. Moreover, for comparison Fig. 6 (a) also shows the enthalpy for MC simulation starting with both structures (bcc and fcc). Therefore, there is a minimum for 700K with a value −0.1 eV much more negative than the one seen for the MC simulation starting from a bcc type-structure (−0.02 eV) indicating a much more stable final configuration. Analyzing Fig. 6 (b), it can be observed that the difference between free energy is negative above 1300K which indicates that a segregated phase should occur below this temperature and a single solid solution should be formed at higher temperatures.

The XRD simulation of the polycrystal resulting from MD simulation at 300K starting from fcc type-structure is shown in Fig. 7 (a). The pattern is typical of a bcc crystal structure with a lattice parameter of about 3.05 Å, albeit again the splitting of the peak around 60° can be interpreted as a tetragonal distortion, as in Fig. 3 (a).

The XRD simulation of the whole alloy from MC simulation at 300K

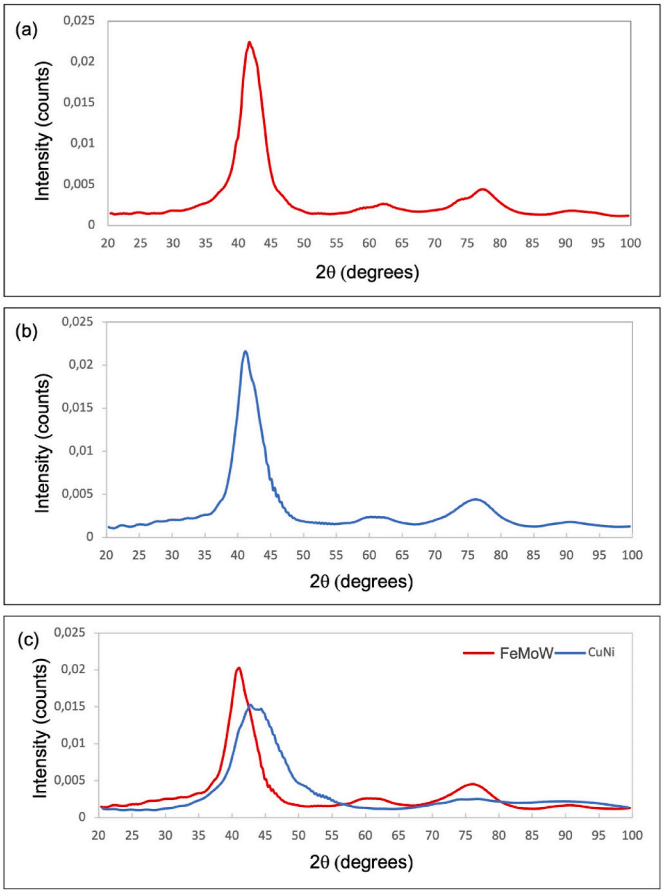

Fig. 7. –XRD for simulations starting with a fcc type-structure at 300K for (a) MD of the polycrystal, (b) MC with XRD of whole Cu–Fe–Ni–Mo–W polycrystalline alloy, (c) MC with XRD of the two phases obtained separately.

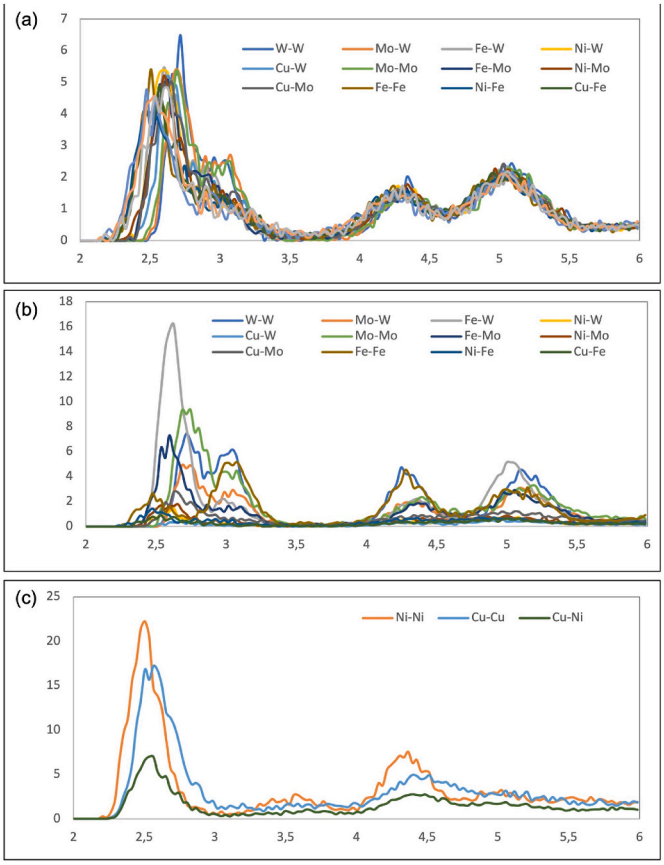

Fig. 8. RDFs of simulations starting from fcc type-structure at 300K for (a) MD simulation resulting in bcc type-structure, (b) MC simulation major bcc W–Fe–Mo phase and (c) MC simulation minor fcc Ni–Cu phase.

starting from fcc, presented in Fig. 7 (b), yielded an asymmetric first peak but essentially consistent with a bcc crystal structure with a lattice parameter of about 3.077 Å. However, if the XRD patterns of both phases are simulated separately (Fig. 7 (c)), it is observed that the Cu–Ni phase has a quite broad peak, but the fcc type-structure with lattice parameter ~3.60 Å is quite different from that of Fe–Mo–W bcc phase with lattice parameter ~3.08 Å, hence the asymmetry of the sum peak in Fig. 7(b).

The RDFs of the MD simulation starting from fcc type-structure at 300K is presented in Fig. 8 (a) and are typical of a bcc type-structure albeit being sourced in a polycrystal simulation cell. In contrast, the RDFs of the MC simulation starting from fcc type-structure at 300K show two phases quite distinct, typical of bcc and fcc type-structures, respectively Fig. 8 (b) and (c), confirming that the chemical segregation of a Ni–Cu phase matches a fcc crystal structure for the MC simulation. It can be concluded that the choice of starting structure is decisive for achieving the lowest energy configuration. In the present alloy it seems that the nucleation of a fcc phase in a bcc matrix is rather difficult and induces a very distorted bcc structure to accommodate the chemical phase separation. Conversely when starting from a fcc matrix the nucleus for the minor fcc is already available and the transformation of the major phase to bcc proceeds with ease. Nevertheless, there is always a significant dispersion of first neighbor distance in Fe–Mo–W (Fig. 8 (b)), typical of HEAs. The simulation results indicate that it much easier to nucleate a less compact structure (bcc) from fcc than the opposite even when the MC procedure is used. In general, a phase transition simulation, such as fcc-bcc, using the Metropolis Monte Carlo method involves an intermediate situation of "entropic barrier" that may require special techniques to proceed [31]. Using molecular dynamics simulation there is evidence that the fcc-bcc transformation proceeds using known

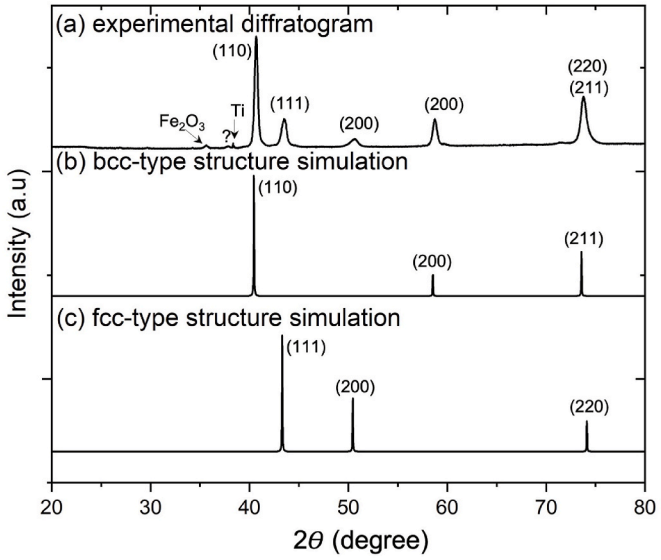

Fig. 9. a) Experimental diffractogram of the Cu–Fe–Mo–Ni–W multi-component produced by arc furnace together with the (b) bcc and (c) fcc type-structure simulations. The peaks at small angles were identified as Fe_2O_3 and Ti and a non-identified one.

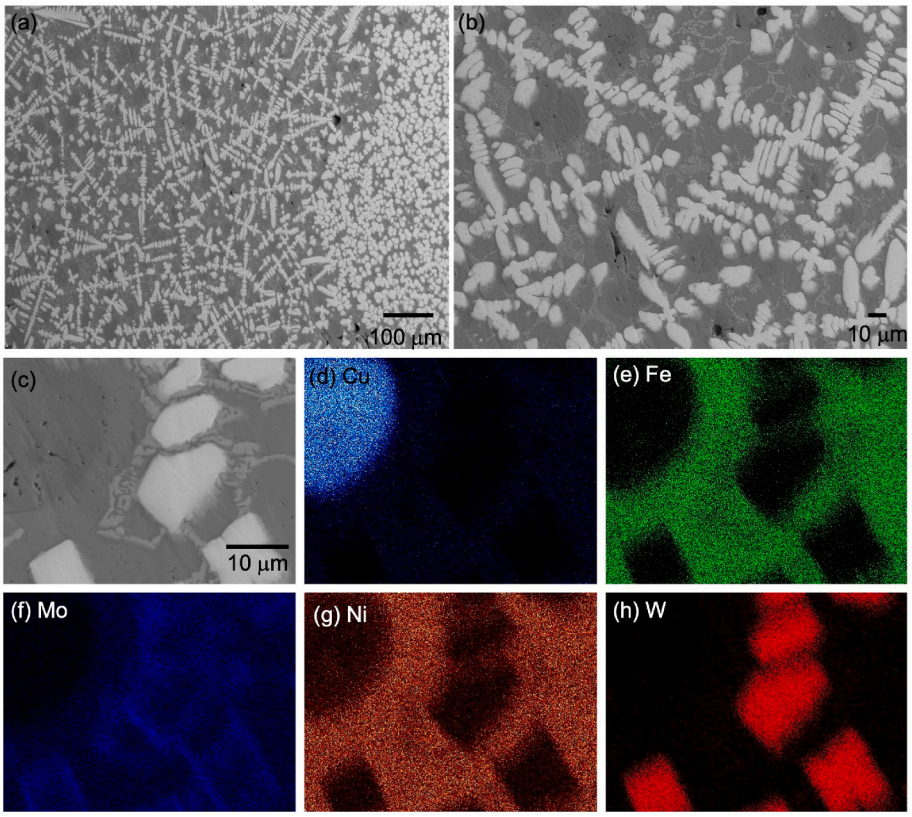

Fig. 10. (a),(b) and (c) SEM images showing the microstructure of the samples produced by arc furnace. EDS map of figure (c) for different elements: (d) Cu-Kα, (e) Fe-Kα, (f) Mo-Lα, (g) Ni-Kα, and (h) W-Mα X-ray lines.

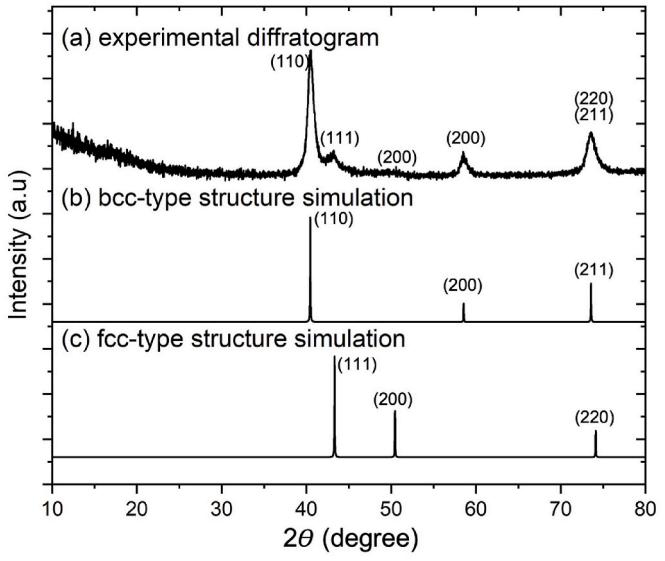

Fig. 11. Experimental diffractograms of the Cu–Fe–Mo–Ni–W multi-component (a) of the milled powder together with the (c) fcc and (d) bcc type-structures simulations.

orientation relationships between both lattices similar to those in martensitic transformations [32].

3.4. Experimental production of the alloy

In the next section, two types of synthesis of the Cu–Fe–Mo–Ni–W multi-component will be presented and discussed. Fig. 9 shows the experimental diffractogram of the Cu–Fe–Mo–Ni–W multi-component sample produced by arc furnace. The results indicate the presence of the peaks of a major bcc type-structure phase with a lattice parameter of 3.14 Å and a minor fcc type-structure one 3.61 Å (close to that of pure Cu). Moreover, Fig. 10 exhibit the microstructure of the Cu–Fe–Mo–Ni–W multi-component produced by arc furnace. The microstructure evidences two distinct regions: a dendritic and an interdendritic one. The EDS map shows that the dendrites correspond to a W–Mo rich regions (Fig. 10 (h)) while the interdendritic regions have the remaining elements. In these regions a binary eutectic was identified as well as Cu segregated phase. In fact, the fcc type-structure found in X-ray results (Fig. 9) seems to agree with the Cu-rich phase found in the microstructure observation (Fig. 10). However, the formation of Cu–Ni phase as was predicted by simulation is not evident. The formation of Cu–Ni phase is expectable since the two elements are of similar atomic size and have the same fcc structure as was published on [33]. Nevertheless, during the preparation by arc-melting of the Cu–Fe–Mo–Ni–W alloy, phase separation is expected can occur owing to the extreme difference in melting temperature of the constituting elements, ranging from Cu (1358K) to W (3680K). Thus this technique is unable to achieve thermodynamic equilibrium which means that metastable phases can be obtained.

The powders were also milled and the experimental diffractogram of the Cu–Fe–Mo–Ni–W multi-component milled is shown in Fig. 11 together with the fcc and bcc type-structure simulations. The diffractogram indicates the presence of a major phase with a bcc type-structure with a lattice parameter of 3.15 Å and a minor phase with a fcc type-structure with a lattice parameter of 3.61 Å, which is similar to what was found for the samples produced by arc furnace. This value for the fcc type-structure is close to the one of the intermetallic proposed by MC simulation starting with a bcc type-structure: Cu–Ni intermetallic has a fcc type-structure and a lattice parameter of 3.56 Å.

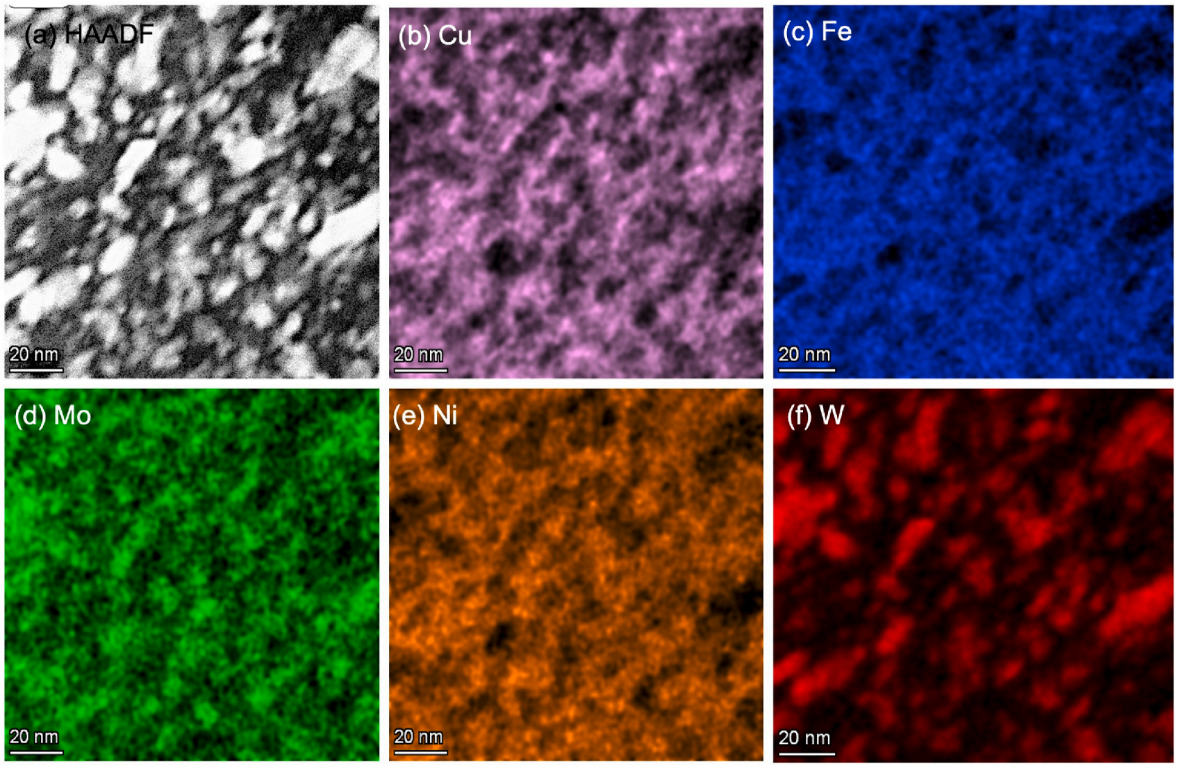

Fig. 12. (a) TEM images of the powder of Cu–Fe–Mo–Ni–W multi-component milled powder together with the EDS maps for (b) Cu-Kα, (c) Fe- Kα, (d) Mo-Kα, (e) Ni-Kα and (f) W-Mα X-ray lines.

Moreover, the lattice parameters predicted for the formation of a bcc type-structure at 300 K, derived directly from the size of the simulation cells, was 3.08 Å for MC starting from fcc, 3.01 Å for MC starting with bcc and 3.02 Å for MD which are discrepant from those observed for the sample produced by arc furnace (a = 3.14 Å) and by milling (a = 3.15 Å). The simulation results albeit far from perfectly predicting the constitution of the alloy evidence the superior achievement of the hybrid MC over the pure MD. In HEAs with many transition elements, the low diffusion rate and the practical time span available for the MD simulation process hinders the achievement of most stable configuration. The introduction of MC swaps overcomes these physical limitations within the available simulation time span. Therefore, the hybrid Monte Carlo simulation proved a superior method to the plain MD simulation as it predicted phase separation of the same elements as detected experimentally while using the same EAM potential.

Fig. 12 shows the TEM images of the powder after milling together with the EDS elemental map for all the elements present in the Cu–Fe–Mo–Ni–W multi-component alloy. As can be observed the powder have a very small grain size (around 20 nm) and the particles are not homogeneous in composition. The EDS map revealed that some particles are only W–Mo rich while the others are Cu–Fe–Ni rich. In fact, the separation after milling seems to be associated with the difference of the melting points of the elements, W and Mo have high values and the transition metals Cu–Fe–Ni have the low ones. This can be rationalized considering that in mechanical alloying both plastic deformation and heating due to collisions play a role in the blending of the elements. The higher melting point metals, notably W, hinder the process of metal blending, i.e. tend to be excluded from the overall multicomponent alloy via mechanisms related to the high melting point of this metal. Firstly, W experiences fast work hardening and does not recover below 873K [32], unlike most transition metals. It therefore remains in the form of hard inclusions [34]. Secondly, the activation energy for diffusion also correlates with the melting temperature of the metal [35]. Hence the local heating due to collisions of the milling media is much less effective as promoting interdiffusion when a high melting point metal such as W is present. The atomistic simulations are in general designed for overall energy minimization. In particular those involving MC processes can achieve the system lowest values of potential energy without resorting to diffusion mechanisms to proceed [31]. It is therefore not surprising that with MC simulation slightly different phase constitution results are obtained relative to those seen experimentally either with melting or milling. Moreover, the MC simulation results are an indication of possible minimum energy alloy constitution notwithstanding practical difficulties such as very different activation energies, amongst the different elements present in the alloy, for processes such as diffusion or annealing.

Since the results do not point to the formation of a single solid solution, the experimental results are in agreement with thermodynamic calculations presented in Section 2. The enthalpy of mixing and the atomic size difference can only indicates the possibility of the formation of a solid solution, however these two parameters are not sufficient requirements. Phase separation and the intermetallic formation are two factors that hinder the solid solution formation in HEAs. Moreover, the results show that the predictions based on molecular dynamics are also not in agreement with the thermodynamic calculations, since the formation of a single solid solution did not occur using this method.

Hybrid simulation (MC) results starting with a bcc type-structure are closer to those obtained experimentally regarding a chemical phase separation, albeit only predicting the presence of a bcc-type structure. In fact, using MC simulation at 300K and starting from a fcc type-structure the Cu–Ni phase obtained has a quite broad XRD peak, but an fcc type-structure can be indexed with a lattice parameter ~3.60 Å which is very close to the experimental one (3.61 Å). In addition, the RDFs from the this phase, presented in Fig. 8 (c), clearly indicate a fcc type-structure. In contrast, the lattice parameter of Fe–Mo–W with the MC starting with bcc type-structure phase obtained is ~3.08 Å, which is quite different from that measured experimentally (3.15 Å).

The MC starting with a fcc type-structure result for the major phase is

the closest to that seen experimentally (3.15 Å) for the bcc phase formation. In contrast with the simulation starting from a bcc type-structure, both for MC (3.01 Å) and MD (3.02 Å). The phase separation obtained in MC method starting with a fcc (W–Fe–Mo and Cu–Ni) is not in agreement with the TEM results (W–Mo and Cu–Fe–Ni) from the milled powder. However, since the simulations were calculated for the thermodynamic equilibrium, it is expected that the phase separation to be different from that of powders milled at room temperature. Moreover, the slight discrepancy in lattice parameter with experimental values, even for the MC starting with a fcc type-structure, is probably the result of the approximation of the EAM potential that cannot match the precision of ab-initio methods such as density functional theory (DFT) [36]. However, the MC simulation used is able to simulate a very large cell, unlike DFT, and the discrepancies in lattice parameter and phase constitution relative to those of the experimental results seem acceptable for a non ab-initio simulation.

4. Conclusions

The stability of the prospective Cu–Fe–Mo–Ni–W multicomponent alloy was tested using MD and MC simulation from 10K to the melting point of the alloy, about 2500K. The choice of starting structure is decisive for achieving the lowest energy configuration. Moreover, the experimental studies are also presented and compared with the simulation.

- With MD only a uniform solid solution was obtained whereas using MC simulation generally produced chemical segregation, i.e. a two phase mixture. In the present alloy the nucleation of a fcc phase in a bcc matrix is rather difficult. Conversely, when starting from an fcc matrix the nucleus for the minor fcc phase is already available and the transformation of the major phase to bcc proceeds.
- Starting the simulation from a fcc-type structure provided both a more stable final configuration and phase separation results closest to those seen experimentally. The potential energy and enthalpy of both types of simulation (MD and MC) versus temperature shows a crossover with MC simulated structures more stable at low temperatures. Starting from fcc, the free energy difference between the two simulated structures, uniform solid solution (MD) versus separation into two phases (MC) indicates phase separation at low temperatures whereas a true HEA is predicted above 1300K.
- The experimental results show that the sample produced by arc furnace exhibit a microstructure with a W-rich dendric phase and a interdendritic Cu segregation while the milled powder evidence an even powder mixture. Both samples show phase separation in XRD, with the formation of bcc and fcc type-structures. It can be concluded that the experimental results are closer to what was observed with the MC simulation starting from a fcc type-structure, since separation into two phases bcc and fcc was correctly predicted.

Declaration of competing interest

The authors declare the following financial interests/personal relationships which may be considered as potential competing interests: Marta Dias reports financial support was provided by Instituto Superior Técnico, Universidade de Lisboa. Marta Dias reports a relationship with Instituto Superior Técnico that includes: employment. No conflict of interests.

Data availability

Data will be made available on request.

Acknowledgements

This work was partially supported by FCT through the contract UID/Multi/04349/2020. The present IPFN activities received financial support from “Fundação para a Ciência e Tecnologia”, Portugal, through projects UID/FIS/50010/2020 and PTDC/FIS-PLA/31629/2017.

References

[1] C.-J. Tong, et al., Mechanical performance of the Al x CoCrCuFeNi high-entropy alloy system with multiprincipal elements, Metall. Mater. Trans. A 36 (5) (May 2005) 1263–1271.
[2] C.-Y. Hsu, J.-W. Yeh, S.-K. Chen, T.-T. Shun, Wear resistance and high-temperature compression strength of Fcc CuCoNiCrAl0.5Fe alloy with boron addition, Metall. Mater. Trans. A 35 (5) (May 2004) 1465–1469.
[3] P.-K. Huang, J.-W. Yeh, T.-T. Shun, S.-K. Chen, Multi-principal-element alloys with improved oxidation and wear resistance for thermal spray coating, Adv. Eng. Mater. 6 (12) (Feb. 2004) 74–78.
[4] Y.Y. Chen, U.T. Hong, H.C. Shih, J.W. Yeh, T. Duval, Electrochemical kinetics of the high entropy alloys in aqueous environments - a comparison with type 304 stainless steel, Corrosion Sci. 47 (11) (2005) 2679–2699.
[5] O. El-Atwani, et al., Outstanding radiation resistance of tungsten-based high-entropy alloys, Sci. Adv. 5 (3) (Mar. 2019) eaav2002.
[6] M.-H. Tsai, et al., Thermal stability and performance of NbSiTaTiZr high-entropy alloy barrier for copper metallization, J. Electrochem. Soc. 158 (11) (Jan. 2011) H1161.
[7] S.A. Kube, S. Sohn, D. Uhl, A. Datye, A. Mehta, J. Schroers, Phase selection motifs in High Entropy Alloys revealed through combinatorial methods: large atomic size difference favors BCC over FCC, Acta Mater. 166 (Mar. 2019) 677–686.
[8] I. Toda-Caraballo, P.E.J. Rivera-Díaz-del-Castillo, A criterion for the formation of high entropy alloys based on lattice distortion, Intermetallics 71 (Apr. 2016) 76–87.
[9] J.-W. Yeh, Recent progress in high-entropy alloys, Eur. J. Control - EUR J Control 31 (Dec. 2006) 633–648.
[10] O.N. Senkov, G.B. Wilks, D.B. Miracle, C.P. Chuang, P.K. Liaw, Refractory high-entropy alloys, Intermetallics 18 (9) (Sep. 2010) 1758–1765.
[11] O.N. Senkov, G.B. Wilks, J.M. Scott, D.B. Miracle, Mechanical properties of Nb25Mo25Ta25W25 and V20Nb20Mo20Ta20W20 refractory high entropy alloys, Intermetallics 19 (5) (May 2011) 698–706.
[12] T.P. Yadav, S. Mukhopadhyay, S.S. Mishra, N.K. Mukhopadhyay, O.N. Srivastava, Synthesis of a single phase of high-entropy Laves intermetallics in the Ti–Zr–V–Cr–Ni equiatomic alloy, Phil. Mag. Lett. 97 (12) (Dec. 2017) 494–503.
[13] V.K. Pandey, et al., Synthesis, characterization and thermal stability of nanocrystalline MgAlMnFeCu low-density high-entropy alloy, Trans. Indian Inst. Met. 74 (1) (Jan. 2021) 33–44.
[14] P. Pradhan, Y. Shadangi, V. Shivam, N.K. Mukhopadhyay, Powder metallurgical processing of CrMnFeCoMo high entropy alloy: phase evolution, microstructure, thermal stability and mechanical properties, J. Alloys Compd. 935 (2023), 168002.
[15] B.S.L. Prasad, A.R. Annamalai, Tungsten heavy alloys with molybdenum, Y2O3 and lanthanum. A review, J. Superhard Mater. 41 (1) (Jan. 2019) 1–16.
[16] L. Xie, P. Brault, A.L. Thomann, J.-M. Bauchire, AlCoCrCuFeNi high entropy alloy cluster growth and annealing on silicon: a classical molecular dynamics simulation study, Appl. Surf. Sci. 285P (Sep. 2013) 810–816.
[17] B. Jelinek, et al., Modified embedded atom method potential for Al, Si, Mg, Cu, and Fe alloys, Phys. Rev. B 85 (24) (Jun. 2012), 245102.
[18] A. Sharma, P. Singh, D.D. Johnson, P.K. Liaw, G. Balasubramanian, Atomistic clustering-ordering and high-strain deformation of an Al0.1CrCoFeNi high-entropy alloy, Sci. Rep. 6 (1) (Aug. 2016), 31028.
[19] M. Widom, W.P. Huhn, S. Maiti, W. Steurer, Hybrid Monte Carlo/molecular dynamics simulation of a refractory metal high entropy alloy, Metall. Mater. Trans. A 45 (1) (Jan. 2014) 196–200.
[20] S. Plimpton, Fast Parallel Algorithms for Short-Range Molecular Dynamics, 1995.
[21] S.P. Coleman, D.E. Spearot, L. Capolungo, Virtual diffraction analysis of Ni [0 1 0] symmetric tilt grain boundaries, Model. Simulat. Mater. Sci. Eng. 21 (5) (Jul. 2013), 055020.
[22] https://www.ctcms.nist.gov/potentials/, "NIST.".
[23] X.W. Zhou, R.A. Johnson, H.N.G. Wadley, Misfit-energy-increasing dislocations in vapor-deposited CoFe/NiFe multilayers, Phys. Rev. B 69 (14) (Apr. 2004), 144113.
[24] C.A. Becker, F. Tavazza, Z.T. Trautt, R.A. Buarque de Macedo, Considerations for choosing and using force fields and interatomic potentials in materials science and engineering, Curr. Opin. Solid State Mater. Sci. 17 (6) (Dec. 2013) 277–283.
[25] S. Guo, C.T. Liu, Phase stability in high entropy alloys: formation of solid-solution phase or amorphous phase, Prog. Nat. Sci. Mater. Int. 21 (6) (2011) 433–446.
[26] Y. Zhang, Y.J. Zhou, J.P. Lin, G.L. Chen, P.K. Liaw, Solid-solution phase formation rules for multi-component alloys, Adv. Eng. Mater. 10 (6) (2008) 534–538.
[27] C. Lee, et al., Lattice distortion in a strong and ductile refractory high-entropy alloy, Acta Mater. 160 (2018) 158–172.
[28] H.S. Oh, et al., Lattice distortions in the FeCoNiCrMn high entropy alloy studied by theory and experiment, Entropy 18 (9) (2016) 1–9.
[29] W. Guo, W. Dmowski, J.-Y. Noh, P. Rack, P.K. Liaw, T. Egami, Local atomic structure of a high-entropy alloy: an X-ray and neutron scattering study, Metall. Mater. Trans. A 44 (5) (May 2013) 1994–1997.
[30] A. Stukowski, “Visualization and Analysis of Atomistic Simulation Data with OVITO – the Open Visualization Tool,”, 2010, 015012.
[31] T.L. Underwood, G.J. Ackland, Lattice-switch Monte Carlo: the fcc - bcc problem, J. Phys. Conf. Ser. 640 (1) (2015).

[32] D. Brunner, "Peculiarities of Work Hardening of High-Purity Tungsten Single Crystals below 800 K,", vol. 389, 2004, pp. 167–170.
[33] R. Rawat, et al., Formation of Cu-Ni enriched phases during laser processing of non-equiatomic AlSiCrMnFeNiCu high entropy alloy nanoparticles, J. Alloys Compd. 927 (Dec. 2022), 166905.
[34] F. Ren, W. Zhu, K. Chu, C. Zhao, Tribological and corrosion behaviors of bulk Cu e W nanocomposites fabricated by mechanical alloying and warm pressing, J. Alloys Compd. 676 (2016) 164–172.
[35] E. R. S. M. Gupta, Devendra, *Diffusion Processes In Advanced Technological Materials*.
[36] M.C. Gao, D.E. Alman, Searching for Next Single-phase High-Entropy Alloy Compositions, 2013, pp. 4504–4519.